# DRAFT SF 298

| 1. Report Date (dd-mm-yy) | 2. Report Type | 3. Dates covered (from... to ) |
|---|---|---|
| 4. Title & subtitle<br>Topographic Radioscopic Metrology for Corrosion Mapping<br>Tri-Service Committee on Corrosion Proceedings | | 5a. Contract or Grant #<br>5b. Program Element # |
| 6. Author(s)<br>John C. Brausch | | 5c. Project #<br>5d. Task #<br>5e. Work Unit # |
| 7. Performing Organization Name & Address | | 8. Performing Organization Report # |
| 9. Sponsoring/Monitoring Agency Name & Address<br>Tri-Service Committee on Corrosion<br>USAF WRIGHT-PATTERSON Air Force Base, Ohio 45433 | | 10. Monitor Acronym<br>11. Monitor Report # |
| 12. Distribution/Availability Statement<br>Approved for Public Release<br>Distribution Unlimited | | |
| 13. Supplementary Notes | | |
| 14. Abstract<br> | | |
| 15. Subject Terms<br>Tri-Service Conference on Corrosion | | |

| Security Classification of | | | 19. Limitation of Abstract | 20. # of Pages | 21. Responsible Person (Name and Telephone #) |
|---|---|---|---|---|---|
| 16. Report | 17. Abstract | 18. This Page | | | |
| | | | | | |

# TRI-SERVICE CONFERENCE ON CORROSION




**21-23 JUNE 1994**

**SHERATON PLAZA HOTEL**
**ORLANDO, FLORIDA**

# PROCEEDINGS

# Topographic Radioscopic Metrology for Corrosion Mapping

**John C. Brausch**
**Wright Laboratory, Materials Directorate**
**Wright Patterson A.F.B.**

## INTRODUCTION

Corrosion of aging aircraft is a pivotal concern in today's Air Force as large transport and tanker aircraft are utilized well beyond their intended design life. The C/KC-135 aircraft, built in the late 1950's and early 1960's is currently projected for service through the year 2040. For such geriatric aircraft, corrosion is often the life limiting factor.

Inspection for lap-joint corrosion on the C/KC-135 during depot maintenance has historically been conducted in a quasi-destructive manner. Typically, maintenance personnel inspect fastener lines for visual indications of corrosion i.e. blistering paint, corrosion products, and skin pillowing. If a suspect region is located the fasteners are removed and a section of the skin lap-seam is peeled open for an invasive inspection. This method is both inefficient and costly.

The Aging Aircraft Disassembly and Hidden Corrosion Detection Program[1], conducted at the Oklahoma City Air Logistics Center (OC-ALC) is attempting to identify off-the-shelf nondestructive inspection (NDI) equipment and technologies that can accurately detect and quantify corrosion in fuselage lap-joint structures of the C/KC-135 and E-3 aircraft. OC-ALC requested that the Materials Directorate of Wright Laboratory develop a laboratory metrological tool by which the corrosion on disassembled aircraft fuselage skins can be accurately measured and mapped. This tool would be used to produce the solution set by which the vendor "round-robin" inspections would be graded.

The resulting technique, Topographic Radioscopic Metrology (TRM), exploits the calibrated gray scale of a digitized radioscopic image through image processing.

The resulting "corrosion maps" supply a topographical quantification of material loss due to corrosion.

This paper describes the technique development, the corrosion mapping process, and the technique validation through metallographic analysis.

**BACKGROUND**

Exfoliation and pitting are the two primary forms of corrosion found in the aluminum fuselage lap-joint skin structures of the KC-135. The corrosion process begins by the ingress of water at the seam. The trapped water sets up a corrosion cell between skin sheets. Material loss due to corrosion occurs at the skin interfaces. (Figure 1)

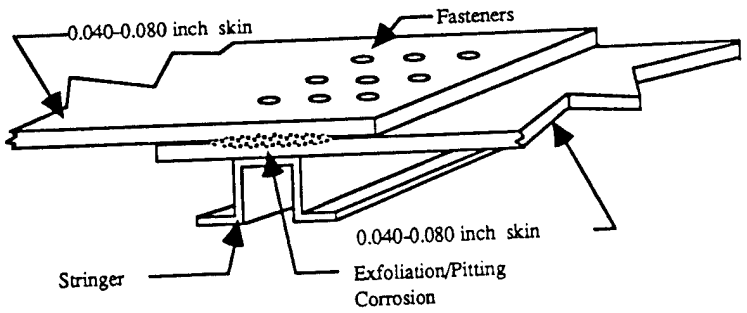


**Figure 1**. Lap-joint corrosion schematic.

Nondestructive methods[2] used for evaluation of material thickness loss due to corrosion include ultrasonic, eddy current and x-radiographic. Immersion ultrasonic and eddy current techniques were evaluated for lap-joint corrosion. However, neither could provide the spatial and thickness resolutions required. Using a focused transducer, in the pulse-echo time-of-flight mode, immersion ultrasonics can produce a two-dimensional representation of skin thickness. However, in the time-of-flight-mode the accuracy of the thickness measurements are limited by the irregular surface contours found in thin lap-joint skins. Immersion ultrasonic techniques are also limited by their slow scan rates. Eddy current techniques are also excellent tools for thickness measurements of flat surfaces. However, due to the nature of eddy currents, the abrupt and irregular thickness changes found in corrosion pits are averaged under the probe footprint resulting in poor thickness resolution.

X-ray imaging is less influenced by these geometric constraints. Therefore, an effort to develop a digitized x-ray imaging technique was conducted.

**THEORY**

If a parallel, monoenergetic beam of X-ray photons is directed against a thin sheet of material, the intensity of the beam will decrease through the thickness of the material according to the law:

$$I = I_o e^{-ux} \quad (3)$$

Where $I_o$ is the incident intensity, $I$ is the transmitted intensity, $x$ is the thickness of the material, and $u$ is a factor called the linear attenuation coefficient. The value of $u$ depends on the energy of the incident photons and the elemental composition of the material. For aluminum at an incident energy of .05 MeV the value for u is 2.448 $in^{-1}$ ($0.964cm^{-1}$)[4]. The transmitted intensity vs. material thickness for aluminum is plotted in Figure 2. As expected the transmitted intensity rises exponentially as the material thickness goes to zero. Over thickness ranges of less than 0.25 inches (0.635 cm) aluminum the curve can be assumed linear.

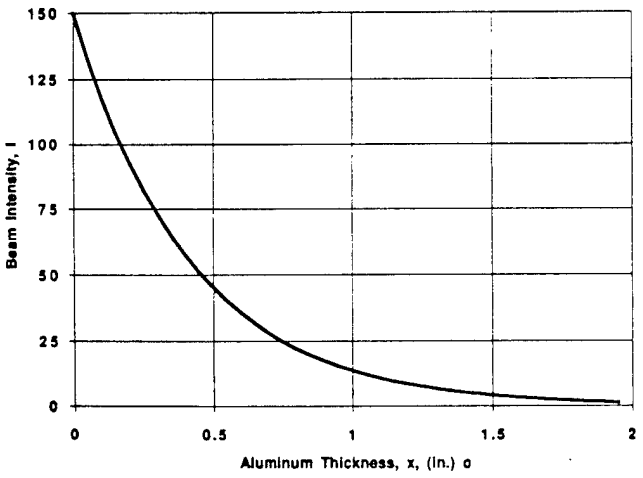


**Figure 2.** Plot of transmitted beam intensity versus material thickness for aluminum.

Variations in x-ray intensity due to differences in material thickness can be recorded via digital x-ray imaging. Measurement of these intensity changes are facilitated through the use of image manipulation software. For digital imaging this relationship can be expressed as the digital image intensity verses the thickness of the material. This "calibration curve" can be determined experimentally through the use of thickness standards milled from the desired material in the ranges of material thicknesses of interest. Each component of an x-ray imaging system (intensifier, camera, processor etc.) may affect this curve, therefore, this curve must be determined for the system as a whole.

## EXPERIMENTAL PROCEDURE

The instrumentation used in this experiment incorporates a FeinFocus 160 kV microfocus x-ray source and a V.J. Technologies 600XDF x-ray intensifier to produce the visible image. A charge coupled device (ccd) camera generates the analog video signal for digitization by a NORAN TN-8502 image processing station (Figure 3).

Specimens can be remotely manipulated for inspection between the x-ray source and image intensifier. The limited detector size allows imaging of only 16 square inches per image. Processing of data for larger areas requires cutting and pasting.

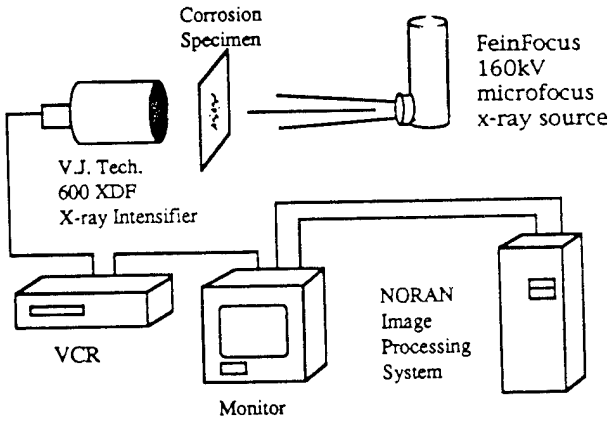


**Figure 3.** Equipment arrangement.

In order to define the calibration curve for relating image intensity to material thickness, thickness standards were manufactured. These standards were milled from 0.040 inch (1.016 mm) 7075-T6 aluminum fuselage skin material to represent material loss values of 2% - 27% (Figure 4). A radioscopic image of these standards was acquired with an exposure of 47 kV and 1.0 mA (Figure 5). The NORAN system captures the intensifier image through 500 frame continuous averaging.

Concentric image patterns caused by the intensity gradients of the x-ray beam are eliminated through digital image subtraction of a background image acquired from a standard of uniform base thickness.

Average pixel intensity measurements were obtained from the center of each step standard. Changes in the average pixel intensity changes were calculated from each step to the next and plotted versus percent material thickness loss as seen in Figure 6. The best fit line for the data set represents the calibration curve by which an image with corrosion may be scaled to derive experimental thickness loss values. Note the Correlation Coefficient (R=0.98739), shows a good fit to linearity. The slope of the calibration curve will be affected by the x-ray energy as well as material thickness. Therefore, this curve must be determined for each specimen inspection series. The experimental thickness losses, calculated via the equation for the best fit line, were compared to thickness losses measured via micrometer. The standard error was calculated to be (+/-) 1.2%; the level of accuracy that can be expected from this method.

(a)

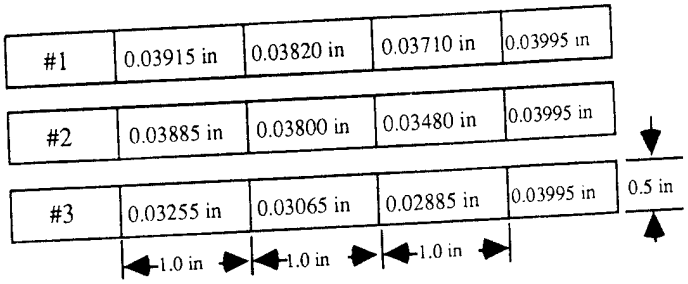


(b)


**Figure 4.** (a) Schematic of machined thickness standards and (b) photograph of standards.


**Figure 5.** Digitized radioscopic image of thickness standards. Image used to determine the calibration curve relating image intensity and percentage material thickness loss.

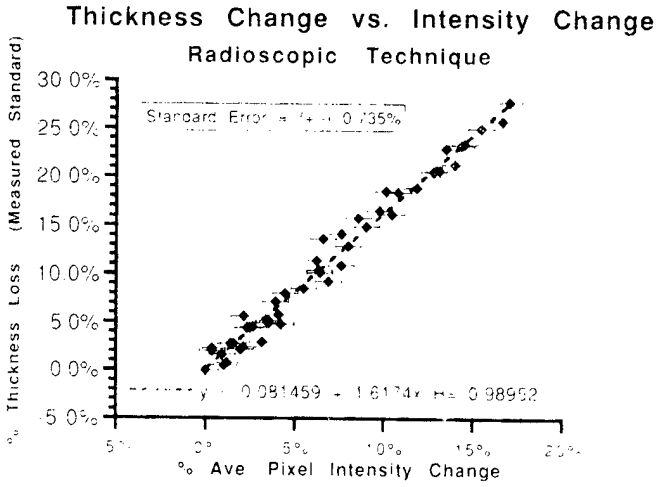


**Figure 6.** Plot of Percent Material Thickness Loss versus Percent Average Pixel Intensity Change.

A radioscopic image of a corroded region (Figure 7) on a 0.040 inch (1.016 mm) 7075-T6 aluminum fuselage lap-joint specimen and a 0.03009 inch (0.764 mm) thickness standard was acquired with an x-ray exposure of 47 kV at 1.0 mA The image was digitally corrected for x-ray beam non-uniformity (Figure 8). Figure 9 represents the histogram of the image of the specimen.

Measuring average pixel intensities for the thickest and thinnest regions (uncorroded base material and thickness standard respectively), provides end points for histogram contrast expansion. The primary peak represents the corrosion specimen and the secondary peak represents the thickness standard. The peaks of these spikes are selected and the data between these peaks are chopped and stretched to fit the TN-8502's full dynamic range of 0 and 256. Colorization of the image is accomplished by dividing the dynamic range by 24 percent (thickness standard) resulting in a 10.4 point intensity change for a 1 percent change in material thickness. Assuming a linear relationship between material thickness and image intensity, the image's histogram is scaled and color banded accordingly. A colorized histogram will appear similar to Figure 10 with the resulting image as shown in Figure 11.

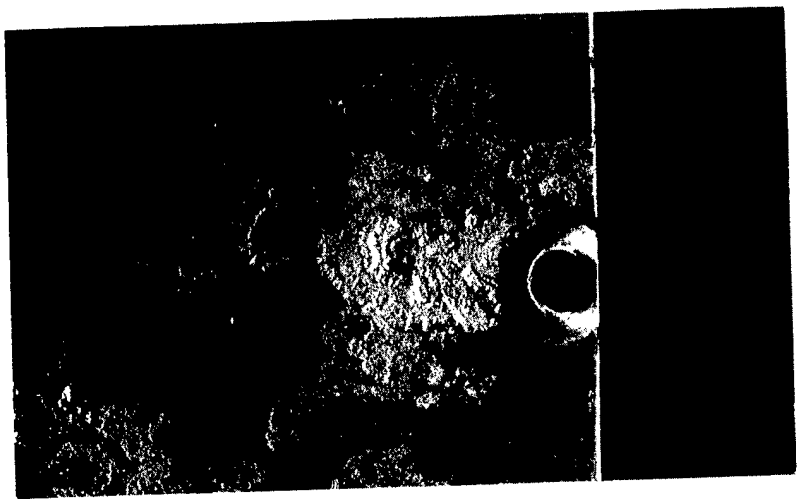

**Figure 7.** Photograph of corrosion site on 0.040 inch (1.016 mm) 7075-T6 aluminum fuselage skin from a C/KC-135.

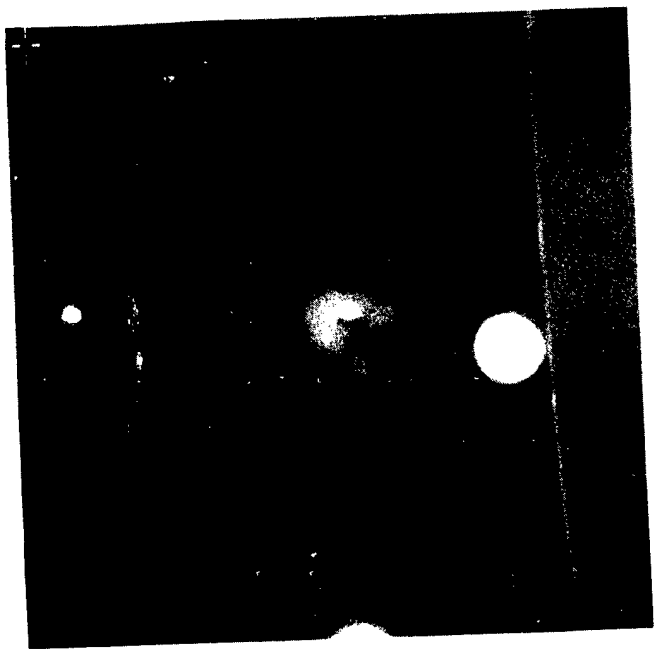

**Figure 8.** Digitized radioscopic image of corroded aluminum specimen. Image is unenhanced.

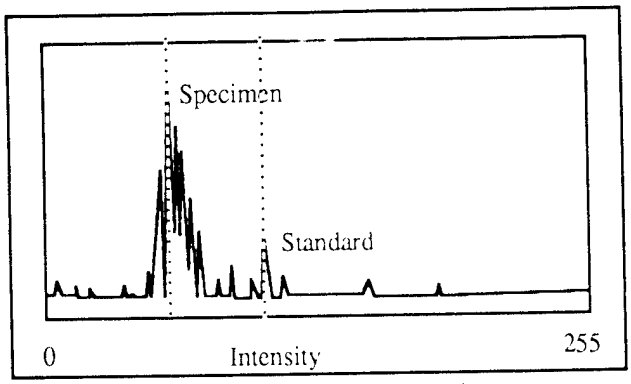


**Figure 9**: Representative histogram of radioscopic image.

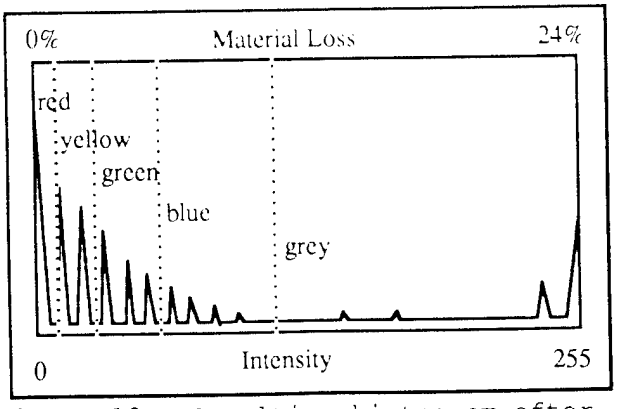


**Figure 10.** Resulting histogram after expansion and color scaling.

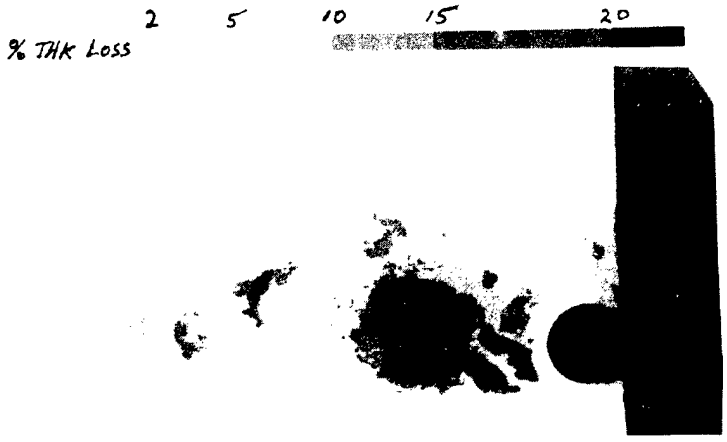


**Figure 11.** Digitized radioscopic image of corroded specimen after contrast expansion, calibration and colorization.

## VALIDATION

Correlation to physical data was achieved through metallographic cross-sectional measurement of the corrosion sites and comparison to topographical data. Again, a colorized topographic map of material thinning of a 0.040 inch (1.016 mm) 7075-T6 aluminum skin was acquired using the method previously described (Figure 12). Two cross-section samples were cut from the corrosion area. These sections were mounted, polished, and percentage thickness losses were microscopically measured along the cross-sectional length. Comparative data are illustrated in Figures 13 and 14 for cross-sections A-A and B-B respectively. It can be seen that the physically measured data correlate very well with the experimental results.

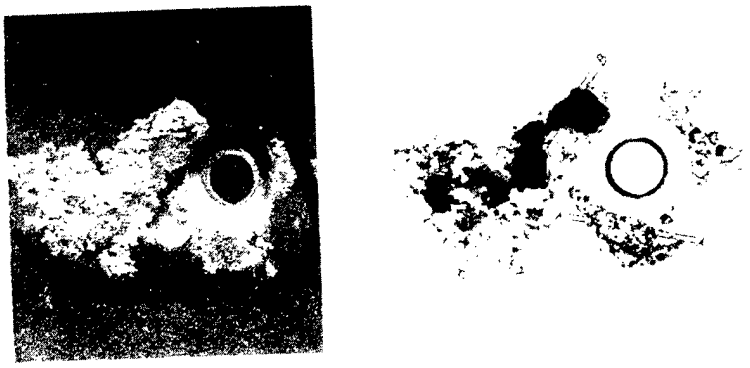

**Figure 12.** Photograph and scaled radioscopic image of a corrosion site on a 0.040 inch (1.016 mm) 7075-T6 aluminum skin. Bars A-A and B-B indicate segments of data forcomparison to physical measurement.

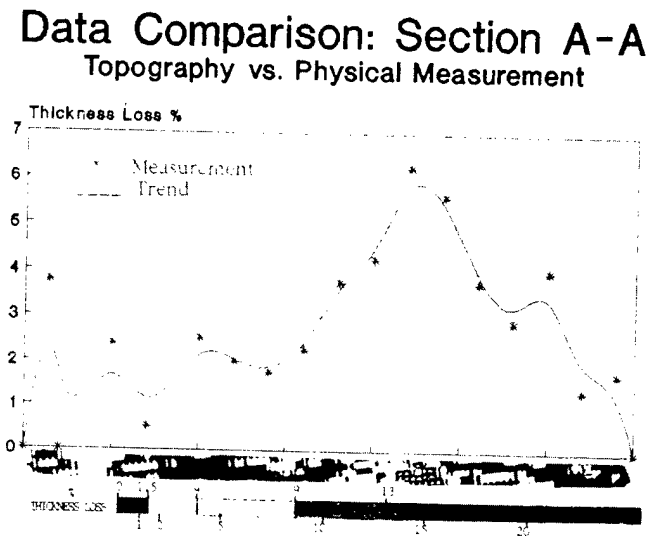


**Figure 13.** Plot of percentage thickness loss for cross-section A-A verses experimental topographical data obtained from Figure 12.

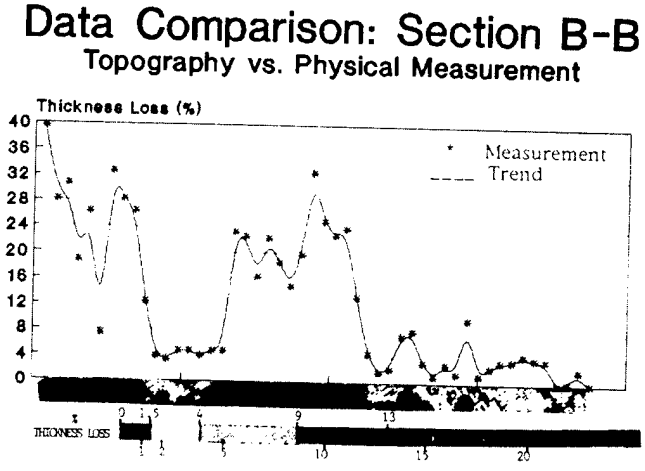


**Figure 14.** Plot of percentage thickness loss for cross-section B-B verses experimental topographical data obtained from Figure 12.

## CONCLUSIONS

Topographic Radioscopic Metrology has demonstrated the ability to quantify and map material thickness losses on the order of 2.0% (+/-)1.2%.

TRM has been shown to be an effective tool for the quantification of thickness changes on thin aluminum sheets. The technique's high spatial resolution make it ideal for accurate quantification and mapping of the complex topography associated with corrosion.

## SUMMARY

Oklahoma City Air Logistics Center identified a need for a nondestructive metrological tool for corrosion quantification of thin aluminum skins associated with fuselage lap-joints.

This paper discussed the development of an x-ray imaging technique, Topographic Radioscopic Metrology, which exploits the calibrated gray scale of a digitized radioscopic image for deriving material thickness values.

The process by which the calibration curve for x-ray image scaling was detailed. The histogram manipulation and colorization scheme was discussed with and an example of corrosion maps given.

Verification of the technique was accomplished through metallographic examination.

## REFERENCES


1. Alcott, J.,"An Investigation of Nondestructive Inspection Equipment: Detecting Hidden Corrosion on USAF Aircraft," *Materials Evaluation* Vol.52, No. 1, Jan.,1994, pp. 64-73.

2. ASTM: G46-92, *Standard Practice for Examination and Evaluation of Pitting Corrosion*, Philadelphia, PA: ASTM, 1993.

3.. Kaelble, E. F., editor, *Handbook of X-Rays for Diffraction, Emission, Absorption and Microscopy*, pp. 1.1-1.31, McGraw-Hill Book Co., New York, 1997.

4. American Society for Nondestructive Testing, *Nondestructive Testing Handbook*, Bryant, L.E., technical editor, McIntire, P, editor, Second Edition, Vol. 3, pg. 846.